PHYSICAL REVIEW C VOLUME 26, NUMBER 4 OCTOBER 1982

Intranuclear cascade calculation of pion-nucleus reactions in the resonance region

Z. Fraenkel
Nuclear Physics Department, Weizmann Institute, Rehovot 76100, Israel

E. Piasetzky and G. Kalbermann
Physics Department, Tel Aviv University, Tel Aviv 69978, Israel
(Received 22 March 1982)

The predictions of the intranuclear cascade model are compared with experimental inclusive pion-nucleus inelastic scattering and absorption cross sections in the Δ-resonance region as a function of bombarding energy and target mass and with the results of recent measurements of $(\pi,\pi p)$ and $(\pi^+,2p)$ for ^{12}C and ^{209}Bi at $E_{lab}=245$ MeV in which the two outgoing particles were measured in coincidence. The calculations reproduce well the mass dependence of the inclusive cross sections; however, the calculated bombarding energy dependence is flatter for the inelastic cross section and more peaked for the absorption cross section than the experimental energy dependence. The calculations for ^{12}C were made with two assumptions regarding the momentum distribution of the nucleons in the nucleus: (1) the "usual" local degenerate Fermi gas; (2) a momentum distribution based on an harmonic-oscillator shell model. The angular correlations for $^{12}C(\pi^+,\pi^+p)$ and $^{12}C(\pi^+,2p)$ are shown to provide a sensitive test for the momentum distribution, with the harmonic-oscillator shell model giving better agreement with the experimental results. The calculations show that multiple scattering of the pion and final state interactions of the outgoing proton contribute approximately equally to the nonquasifree part of the (π^+,π^+p) cross section. The calculated number of nucleons N taking part in the pion absorption process has a rather wide distribution which is generally peaked at the minimum number, $N=2$. The calculated $(\pi^-,\pi^-p)/(\pi^+,\pi^+p)$ cross section ratio for the quasifree peak at 245 MeV is larger than the free ratio in contradiction with the experimental results. This may be an indication of coherent effects which are not included in the intranuclear cascade model.

[NUCLEAR REACTIONS Compared predictions of intranuclear cascade model for pion-nucleus reactions with experimental results for inclusive inelastic scattering and true absorption and for angular correlations for the $(\pi,\pi p)$ and $(\pi^+,2p)$ processes. $E_\pi=85-315$ MeV, $A=7-209$.]

I. INTRODUCTION

The predictions of the intranuclear cascade (INC) model of Chen *et al.*[1,2] and Harp *et al.*[3,4] have so far been compared with experimental spallation residue cross sections and inclusive particle emission cross sections for proton and pion-induced reactions.

Recently, a series of more detailed experiments have been performed on pion-induced reactions, in particular, inelastic scattering and absorption, in which two of the outgoing particles were measured in coincidence.[5-7] The comparison of the predictions of the INC model with these more exclusive experimental results presents a much more stringent test for the model than has been available so far. This is particularly true for the pion absorption process which is the only process included in the model for which no experimental free-particle cross sections are available. The INC model of Harp *et al.* assumes that pion absorption in a complex nucleus proceeds solely through the formation of a Δ resonance

$$\pi+N\rightarrow\Delta\ ,$$

$$\Delta+N\rightarrow 2N\ .$$

This process is believed to be the dominant absorption channel in the Δ-resonance region whereas other channels (such as *s*-wave absorption at lower pion energies and absorption through higher resonances at higher energies) contribute significantly only at energies outside the Δ-resonance region. The experimental results of Altman *et al.*[7] on pion absorption are of particular importance as a test of the INC model of Harp *et al.*, since these experiments were performed in the Δ-resonance region. In addition to testing the validity of the INC model for pion-nucleus reactions, the detailed comparison with the experimental results is expected to yield information on certain parameters of the model such as the pion-nucleus potential and the momentum distribution of the nucleons in the nucleus.

The INC model yields, on the other hand, detailed information on the experimentally investigated reactions, information which, in general, cannot be extracted directly from the experimental results. Thus the questions of the average number of nucleons taking part in the pion absorption process, the importance of multiple pion scattering in the nucleus before absorption, and of the rescattering of the nucleons taking part in the absorption process ("final state interactions") have aroused considerable interest in view of the recent experimental results on pion absorption.[8] The INC model is capable of providing detailed answers to these and other questions relating to pion interactions in the nucleus.

In this paper we describe a comparison between the predictions of the INC model of Harp *et al.*[4] with the experimental results on (1) inclusive inelastic scattering and absorption reactions as a function of the pion energy and the mass of the nucleus,[9] (2) the angular correlations between protons and pions in the (π^+,π^+p) reaction of 245 MeV π^+ on ^{12}C, ^{56}Fe, and ^{209}Bi (Refs. 5 and 6), and (3) the angular correlation between the two outgoing protons in the $(\pi^+,2p)$ absorption of 245 MeV π^+ on ^{12}C, ^{56}Fe, and ^{209}Bi.[7] In Sec. II we discuss briefly the changes made in the INC model as compared to that described previously.[1–4] We present the results of the calculation and the comparison with the experimental results in Sec. III. Section IV contains a brief discussion of the comparison of calculated and experimental results and our conclusions.

II. THE MODEL

The principal features of the INC model, which were used in the present work, have been described in great detail previously.[1–4] We will confine ourselves here only to the description of those aspects in which the present model differs from that of Chen *et al.*[1,2] and Harp *et al.*[3,4] Most of these changes do not affect the results of the calculation very significantly and they were mainly introduced for the sake of consistency within the present model and with the relativistic-heavy-ion version of the model.[10,11]

The more important changes were: (1) The width of the Δ resonance was assumed to be energy dependent. The energy dependence is the same as that described by Ginocchio.[12] (2) A minimum distance was imposed between two consecutive collisions of a given particle. This restriction has been discussed by Chen *et al.*[13] We have used the density-dependent distance restriction[13] for which the minimum distance d between two consecutive collisions of a particle is given by

$$\tfrac{4}{3}\pi d^3\rho(r)=1 ,$$

where $\rho(r)$ is the nuclear density (which changes with the nuclear radius). However, unlike the calculation of Chen *et al.*, the present calculation assumes the distance restriction to be *isospin dependent* (i.e., the distance restriction is assumed to hold only for consecutive collisions of a particle with two protons or two neutrons, but not with a proton followed by a neutron or *vice versa*). This particular distance restriction was used in order to make the model consistent with the relativistic heavy-ion calculation in which a closely similar procedure (isospin-dependent slow-rearrangement) is used to account for depletion of the Fermi sea during the collision.[10] (3) The nuclear density distribution was simulated by a step function distribution with a nuclear radius parameter of $r_0=1.18$ fm.

The most important change introduced in the model concerns the momentum distribution of the nucleons in the nucleus. In all previous calculations this distribution was taken to be the "local" degenerate Fermi gas distribution; i.e., for a given region i with density ρ_i the momentum distribution was that of a local degenerate Fermi gas (LFG) with the Fermi energy

$$E_F=(\hbar^2/2m)(3\pi^2\rho_i)^{2/3} . \quad (1)$$

While it was known that the LFG distribution was probably a poor description of the actual momentum distribution of the nucleons, particularly for light nuclei, the calculations performed so far with the INC model related mostly to experimental results which were not sensitive to the nuclear

momentum distribution. This is not the case for the coincidence experiments mentioned above. As we shall show below, these experiments are a sensitive test of the nuclear momentum distribution and not surprisingly, the INC model with the LFG momentum distribution fails to reproduce the experimental results.

Hüfner and Nemes[14] have pointed out that for a given nuclear radius the momentum distribution of the nucleons is given (within certain limitations; see Ref. 14 for details) by the Wigner transform of the one-body density matrix

$$W(R,p)=\int \frac{d^3x}{(2\pi)^3}\exp(-\vec{p}\cdot\vec{x})\left\langle \vec{R}-\frac{\vec{x}}{2}\left|\rho\right|\vec{R}+\frac{\vec{x}}{2}\right\rangle . \tag{2}$$

For the LFG model this expression has the form[14]

$$W(\vec{R},p)=\rho(\vec{R})\frac{3}{4\pi {p_F}^3(R)}\theta[{p_F}^2(R)-p^2] , \tag{3}$$

where p_F is the Fermi momentum and

$$\theta(x)=\begin{cases}1 & x\geq 0\\ 0 & x<0\end{cases},$$

whereas for the shell model with harmonic oscillator wave functions (SM-HO) the Wigner transform has the analytic expression[14]

$$W(R,k)=\frac{1}{2\pi^3}\left[\frac{R^2}{b^2}+k^2b^2-1\right]\exp\left[-\frac{R^2}{b^2}-k^2b^2\right], \tag{4}$$

where b is the length parameter of the well, and $k=p/\hbar$. In the present work we compare the predictions of the INC model with the LFG momentum distribution and that of the SM-HO momentum distribution for the ^{12}C nucleus. The length parameter of the harmonic oscillator well is $b=1.64$ fm.[15] $W(R,k)$ was calculated separately for the five outer density regions of the nucleus (the inner three regions are of little importance for pion reactions which are predominantly surface reactions; hence, the LFG distribution was always used for these regions). The density distribution and Pauli blocking were left unchanged.

All calculated results for ^{12}C shown in the following sections were obtained with the SM-HO momentum distribution unless otherwise stated. The results for all other nuclei were calculated with the LFG momentum distribution.

III. COMPARISON WITH EXPERIMENTAL RESULTS

In a series of experiments, which have recently been carried out at the Schweizerisches Institut für Nuklearforschung by the Tel Aviv University-Eidgenossiche Technische Hochschule, Zurich-University of Zurich collaboration, the true absorption,[9] the inclusive pion inelastic scattering,[9] the inclusive pion-induced nucleon-knockout reaction,[5,6] and the $(\pi,2N)$ absorption reactions[7] were studied systematically. The energy of the outgoing pion was not measured and all the results to be presented involve an integration over the outgoing pion energy.

A. Comparison with inclusive measurements

The inclusive inelastic differential cross section was measured[9] for six nuclei, ranging from ^{7}Li to ^{209}Bi, at bombarding energies from 85 to 315 MeV for positive pions, and at 125 and 165 MeV for negative pions. In Fig. 1, the measured and calculated inelastic differential cross section for backward angles of 245 MeV positive pions on ^{12}C and ^{209}Be are shown. We restrict our comparison to the backward angles since in this region the contribution of elastic scattering (which is not included in the calculated cross section) is negligible. The calculation

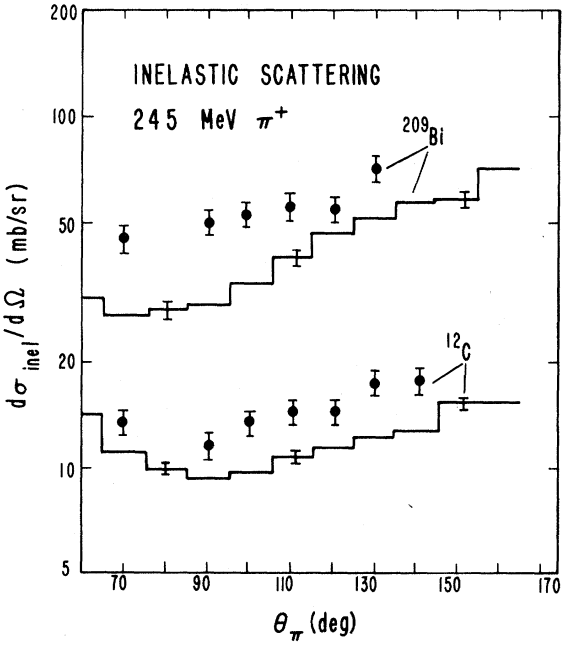

FIG. 1. Differential scattering cross section of 245 MeV π^+ on ^{12}C and ^{209}Bi. The circles denote the experimental results of Ashery *et al.* (Ref. 9) and the histograms denote the results of the INC calculation for inelastic scattering.

reproduces the *shape* of the experimental angular distribution which is similar to the free pion-nucleon scattering but the absolute values of the calculated cross sections are systematically below the experimental ones.

Major reaction channels, namely inelastic scattering (Fig. 2), "true" absorption (Fig. 3), and charge exchange (Fig. 4) are shown as a function of the nuclear mass number for 245 MeV positive pions (a) and as a function of the incoming pion energy (b) and (c) for ^{12}C and ^{209}Be, respectively.

It is seen that the calculated inelastic scattering cross section is below the experimental one for low and high A [Fig. 2(a)]. The experimental energy dependence of the inelastic scattering cross section is well reproduced by the calculations for ^{12}C [Fig. 2(b)]. The experimental inelastic cross section for ^{209}Bi is essentially energy independent [Fig. 2(c)] whereas the calculated cross section shows a peak at the resonance cross section. The experimental A

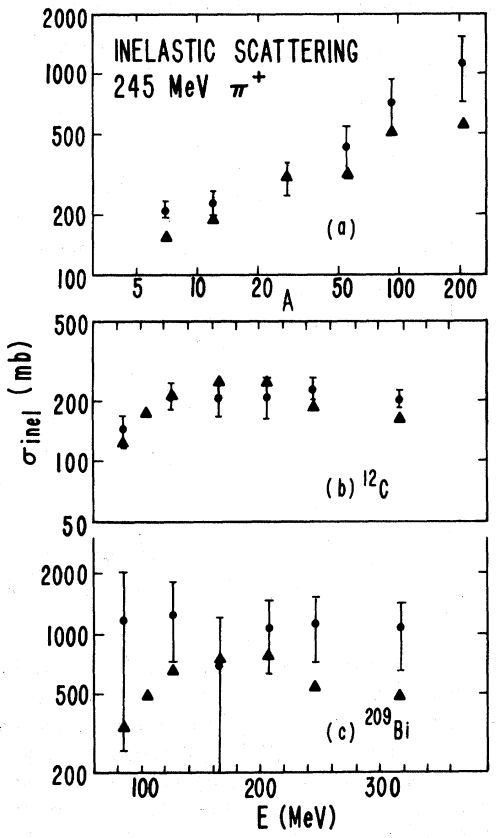

FIG. 2. Total inelastic scattering cross section of π^+ on nuclei (a) as a function of target mass for a pion energy of 245 MeV, (b) and (c) as a function of pion energy for ^{12}C and ^{209}Bi targets, respectively. The circles denote the experimental results of Ashery *et al.* (Ref. 9) and the triangles denote the results of the INC calculation.

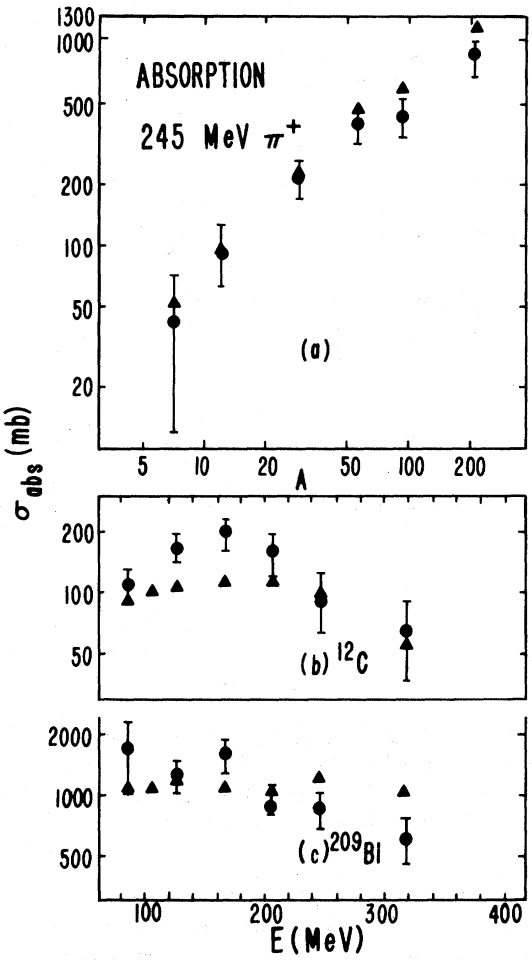

FIG. 3. True absorption cross section of π^+ on nuclei (a) as a function of target mass for a pion energy of 245 MeV, (b) and (c) as a function of pion energy for ^{12}C and ^{209}Bi targets, respectively. The circles denote the experimental results of Ashery *et al.* (Ref. 9) and the triangles denote the results of the INC calculation.

dependence of the absorption cross section is well reproduced by the calculation [Fig. 3(a)] except perhaps for the heaviest nuclei. The energy dependence of the absorption cross section for ^{12}C [Fig. 3(b)] and ^{209}Bi [Fig. 3(c)] shows a trend opposite to that of the inelastic scattering cross section, namely the experimental cross section shows a somewhat sharper peak at the resonance energy than the calculated one.

B. Coincidence measurements of pion-induced proton knockout reactions

Inclusive $(\pi,\pi p)$ reactions on C, Fe, and Bi were studied experimentally[5,6] at 245 MeV over a broad kinematic range by means of coincidence measure-

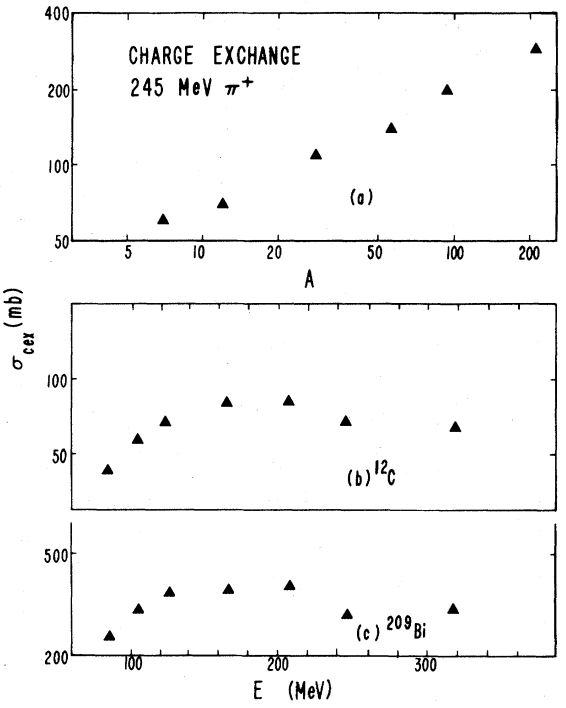

FIG. 4. Calculated charge exchange cross section of π^+ on nuclei (a) as a function of target mass for a pion energy of 245 MeV, (b) and (c) as a function of pion energy for ^{12}C and ^{209}Bi targets, respectively.

ments of the outgoing particles. The π-p angular correlations and proton-energy spectra were measured for backward scattered pions and show features consistent with those expected from quasi-free scattering. Calculated and experimental pion-proton angular correlations for ^{12}C are shown in Fig. 5 for two pion angles, $\theta_\pi = 90°$ and $\theta_\pi = 140°$. The energy spectra of the outgoing proton at the peak of the angular correlation are shown in Fig. 6 for $\theta_\pi = 140°$. The calculations of the angular correlation and the energy spectrum were done with both the LFG and the SM-HO momentum distributions for the nucleons in the ^{12}C nucleus. Both the experimental and the calculated cross sections are restricted to protons emitted in the angular range of $\pm 6°$ with respect to the reaction plane (which is defined by the beam and the direction of the outgoing pion).

It is seen in Fig. 5 that both models reproduce very accurately the peak position of the angular correlation (which is somewhat lower than the free value indicated by the arrow); but whereas the SM-HO calculation shows excellent agreement with the experimental results in both the shape and absolute

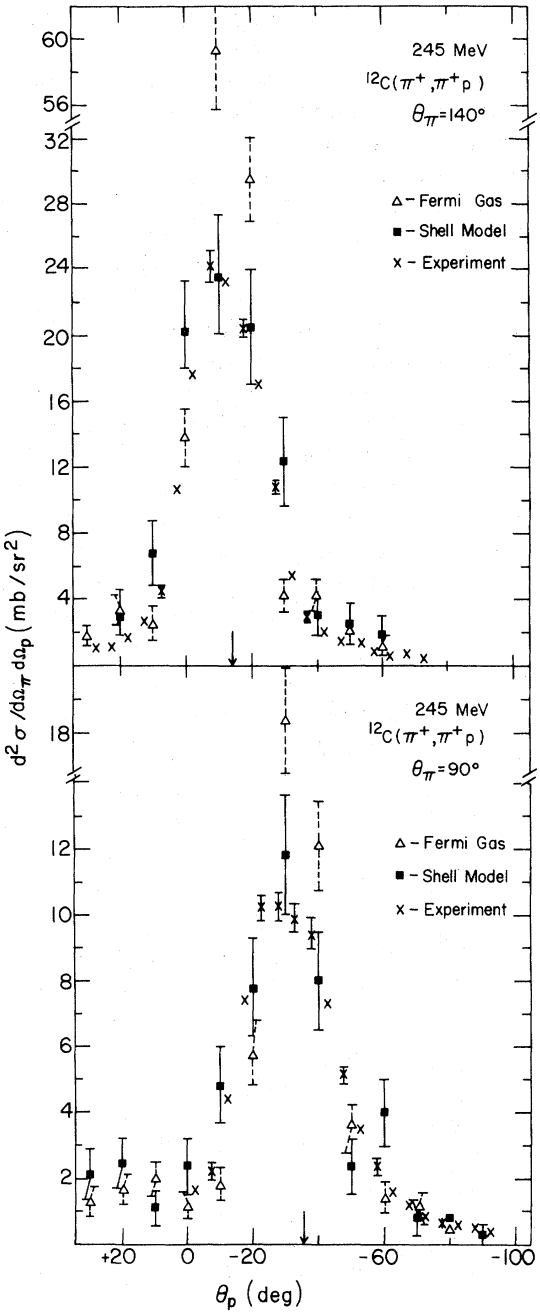

FIG. 5. Pion-proton angular correlations for 245 MeV π^+-induced knockout reaction on ^{12}C for two pion scattering angles. The crosses denote the experimental results of Piasetzky *et al.* (Ref. 5), the squares denote the calculated results for the SM-HO momentum distribution, and the triangles denote the calculated results for the LFG momentum distribution. The arrow marks the free π-p scattering angle.

magnitude of the peak, the LFG model yields a narrower peak of larger amplitude. Similar comments apply to the proton energy distribution (Fig. 6).

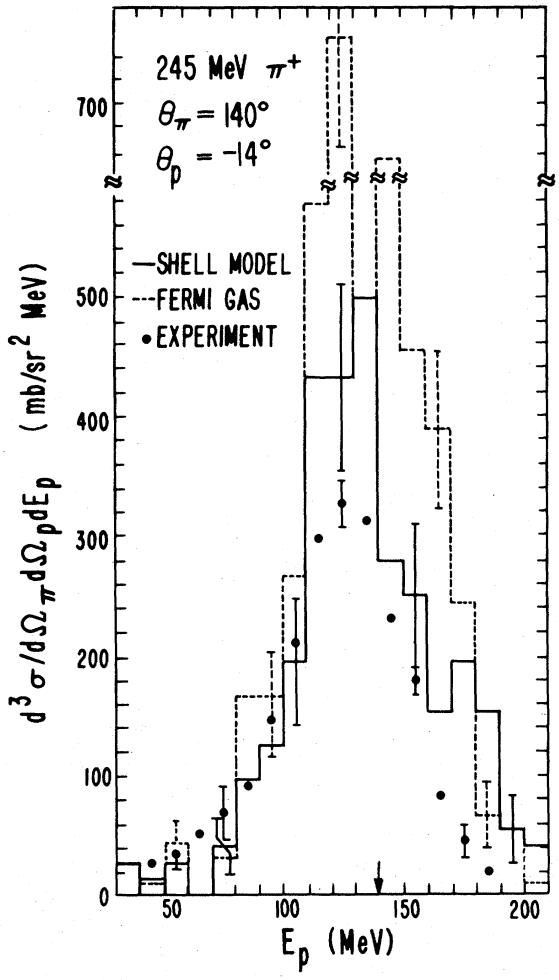

FIG. 6. Energy spectrum of the protons for 245 MeV π^+-induced knockout reaction on ^{12}C for pion and proton scattering angles of 140° and −14°, respectively. The circles denote the experimental results of Piasetzky *et al.* (Ref. 5), the solid-line histograms denote the calculated results for the SM-HO momentum distribution, and the broken-line histograms denote the calculated results for the LFG momentum distribution. The arrow marks the proton energy for free π-p scattering at the above angles.

We show in Fig. 7 the calculated angular correlations of the protons from (π^+,π^+p) and (π^-,π^-p) for 245 MeV pions on ^{12}C for a pion scattering angle of $\theta_\pi = 90°$. The scales for the two correlations differ by a factor equal to the free $(\pi^-,\pi^-p)/(\pi^+,\pi^+p)$ scattering cross section ratio at this energy. It is seen that the calculated peak ratio is somewhat larger than the free one [the statistical errors are however quite large for the (π^-,π^-p) reaction]. This feature does not agree with the experimental result[5] which shows a

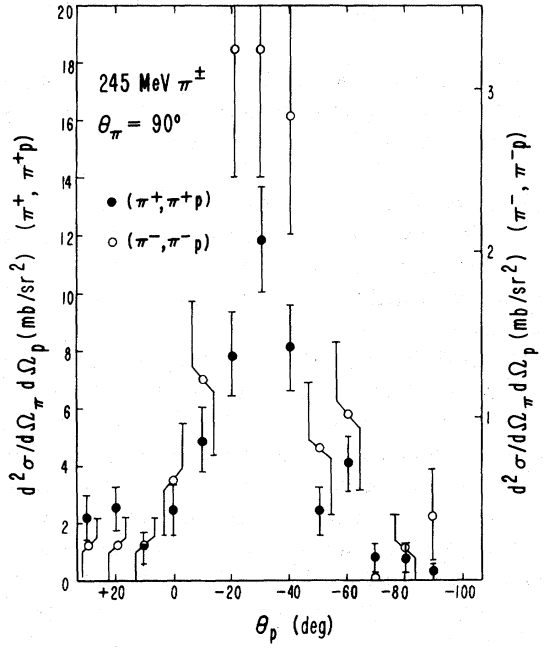

FIG. 7. Calculated pion-proton angular correlations for 245 MeV positive (solid circles) and negative (open circles) pions on ^{12}C at a pion scattering angle of 90°. The scale for π^- scattering (right-hand side) is that for π^+ scattering (left-hand side) multiplied by the ratio of the free π^-p to π^+p scattering cross sections.

$(\pi^-,\pi^-p)/(\pi^+,\pi^+p)$ peak ratio *smaller* than the free value.

C. Coincidence measurements of the $(\pi^+,2p)$ reaction

We show in Fig. 8 the angular correlation of one of the protons in the inclusive $(\pi^+,2p)$ reaction induced by 245 MeV positive pions on ^{12}C. The other proton is detected at an angle of $\theta_{p_1} = 120°$. The figure shows the experimental results of Altman *et al.*[7] and the calculated correlation for both the LFG and the SM-HO momentum distributions. An energy threshold of 80 MeV, equal to the experimental threshold, was imposed on the calculated outgoing protons. As in the case of the previous figures, the experimental and calculated cross sections shown in Fig. 8 pertain to the second proton being emitted in angular range of ±6° with respect to the reaction plane (which in this case is defined by the direction of the beam and the first proton). It is seen that while both calculations reproduce the experimental "quasideuteron" peak position, the SM-HO distribution gives a better fit to the experimental spectrum although both calculations overestimate the peak cross section.

IV. DISCUSSION

The generally good agreement between the results of INC model calculations and the experimental results demonstrated in the previous section gives credence to the belief that this model contains the basic physical aspects of the pion-nucleus interaction. We may, therefore, use the model to obtain more detailed information on various aspects of the interactions which cannot be obtained directly from experiment.

Of equal interest are the points of qualitative disagreement between the calculation and the experimental results which may indicate the existence of more complicated mechanisms which are not included in the present INC model. In this section, we shall first present the information the model yields on the pion-nucleus reaction mechanism and then we shall discuss the discrepancies between the calculation and the measurements and some possible implications.

A. The pion-induced proton-knockout mechanism

The $(\pi,\pi p)$ reaction cross section in nuclei may be divided into a quasifree (QF) part in which the pion makes a single collision with one of the protons of the nucleus and subsequently both particles leave the nucleus without further interaction, and a "background" due to multiple scattering of the pion (MS) and rescattering of the proton before it leaves the nucleus (final state interaction, FSI). The latter two contributions are, of course, not mutually exclusive since there is a large probability for both scatterings to occur in a given pion-nucleus interaction. Experimentally, one can identify the peak in the angular correlation distribution at the free $(\pi,\pi p)$ angle with the quasifree part of the cross section but the experiment cannot determine the relative importance of pion multiple scattering and the proton final-state interaction contributions to the total knockout cross section. This information is, of course, readily available from the calculations.

In Fig. 9 we show the calculated contributions of the quasifree process, pion multiple scattering, and proton final-state interaction for 245 MeV π^+ on ^{12}C, ^{56}Fe, and ^{209}Bi for pion scattering angles of 90° and 140° as fractions of the total (π^+,π^+p) cross sections. (As already mentioned, the three fractions add up to a value greater than 100% since both the MS and FSI parts include the cross section for which both processes take place.) We also show the

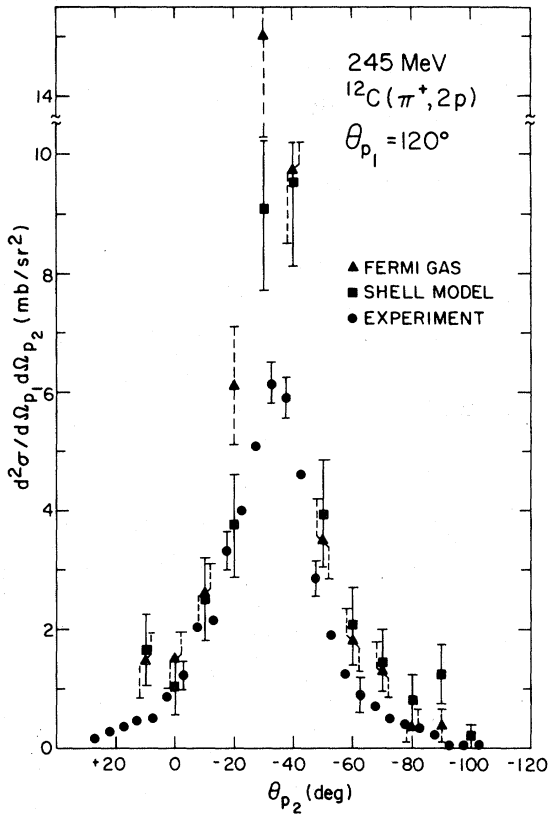

FIG. 8. Proton-proton angular correlation for the inclusive $(\pi^+,2p)$ reaction on ^{12}C at a pion bombarding energy of 245 MeV. The first proton is detected at an angle of 120°. The circles denote the experimental results of Altman *et al.* (Ref. 7), the squares denote the calculated results with the SM-HO momentum distribution, and the triangles denote the calculated results for the LFG momentum distribution.

experimental quasifree fraction which is based on the estimate of the peak area of the angular correlation at the free $(\pi,\pi p)$ angle.[5,6] The experimentally determined quasifree fraction does not show a dependence on the pion scattering angle.

We see from Fig. 9 that, as expected, the quasifree fraction decreases with increasing target mass and that the experimental result is in good agreement with the average calculated value for the two angles. We also see that the MS and FSI mechanisms contribute roughly equally to the "background" of the reaction, but whereas the MS fraction is roughly independent of the target mass A, the FSI increases with increasing A, thus causing the decrease in the QF fraction as a function of A. Finally, the FSI fraction is independent of the pion scattering angle whereas the calculated pion MS fraction decreases with increasing pion angle, thus causing the pion-angle dependence of the calculated

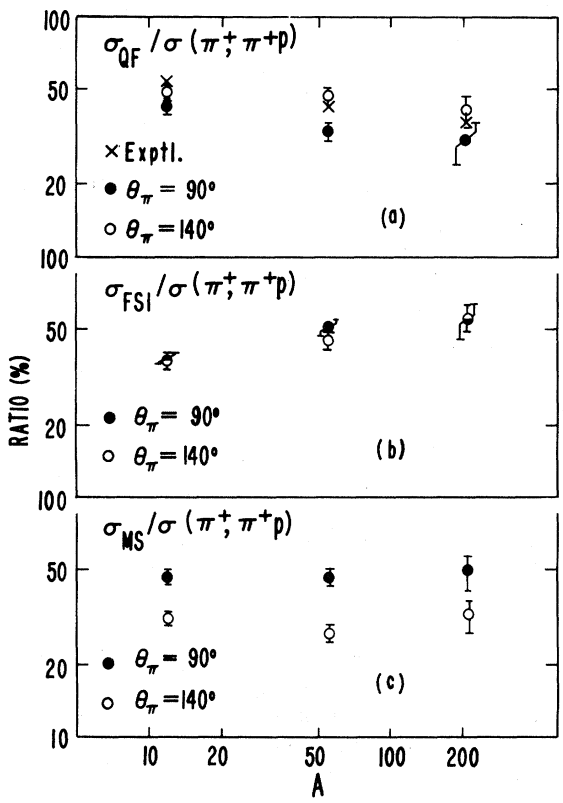

FIG. 9. Calculated partial cross sections for (a) quasifree scattering (QF); (b) final-state interaction of the outgoing proton (FSI); and (c) multiple scattering of the pion (MS) for 245 MeV π^+ on ^{12}C, ^{56}Fe, and ^{209}Bi targets, shown as fractions of the inclusive (π^+,π^+p) cross section for pion scattering angles of 90° (full circles) and 140° (open circles). The experimental estimate of the partial cross section for the quasifree process (which is angle independent) is also shown (crosses). (b) and (c) both include the fraction of the cross section for which both MS and FSI processes occur.

QF fraction.

The above results appear to have a simple geometrical explanation. The calculated average interaction radii for the (π^+,π^+p) reaction on ^{12}C, ^{56}Fe, and ^{209}Bi are 3.6, 5.7, and 8.4 fm, respectively. This means that the π^+-p collision occurs predominantly on the (upstream) surface of the target nucleus. For the heavier nuclei the forward-scattered proton has a longer path to traverse before leaving the nucleus. This effect, together with the larger neutron component in heavier nuclei causes the increase in the proton FSI. The pion, on the other hand, is back scattered from the surface of the nucleus and its path is roughly independent of the nuclear mass but decreases with increasing scattering angle.

Since the pion-induced proton knockout process is a surface reaction, the pion-proton coincidence measurements are sensitive to the momentum distribution of the nucleons in the nuclear surface. At a nuclear radius of 3.6 fm (which is the average interaction radius for ^{12}C), the Fermi momentum for the LFG distribution is $p_F = 125$ MeV/c, whereas the SM-HO momentum distribution for p-shell protons peaks at a value of 160 MeV/c. This is also the value obtained by Belloti *et al.*[16] when they fitted their experimentally measured p-shell proton momentum distribution to the form of Eq. (4). In their experiment Belloti *et al.* measured the (π^+,π^+p) reaction in ^{12}C at 130 MeV using a propane bubble chamber. It is, therefore, not surprising that the LFG distribution, which underestimates the momentum distribution on the nuclear surface, gives poor agreement with the experimental angular correlation, whereas the SM-HO momentum distribution reproduces the experimental results very well (Figs. 5 and 6). Hüfner and Nemes[14] arrived at the same conclusions in their analysis of the (^{16}O, ^{15}O) process at relativistic energies, which is also a surface reaction. Moniz *et al.*[17] determined experimentally the momentum distribution of the protons in the ^{12}C nucleus by means of inelastic scattering of 500 MeV electrons and obtained a value of $p_F = 221$ MeV/c for the Fermi momentum by fitting their experimental results to a Fermi distribution. It should be noted that unlike the (π^+,π^+p) reaction, which is a surface reaction, inelastic electron scattering measures the proton momentum distribution averaged over the whole nuclear volume.

B. The $(\pi^+,2p)$ reaction mechanism

We show in Fig. 10 the calculated inclusive $(\pi^+,2p)$ cross section, the same cross section when lower limits of 80 MeV are imposed on the outgoing protons (which is the lower limit in the experiment of Altman *et al.*[7]) and the direct (i.e., exclusive) $(\pi^+,2p)$ cross section in the interaction of 245 MeV pions with ^{12}C, ^{56}Fe, and ^{209}Bi. The figure shows the ratio of the above cross sections to the calculated total absorption cross section. We see that the inclusive $(\pi,2p)$/(total absorption) ratio equals $\sim$0.5 but decreases somewhat with increasing target mass A. The ratio of the other two cross sections to the total absorption cross section decreases much more sharply with increasing A, as a

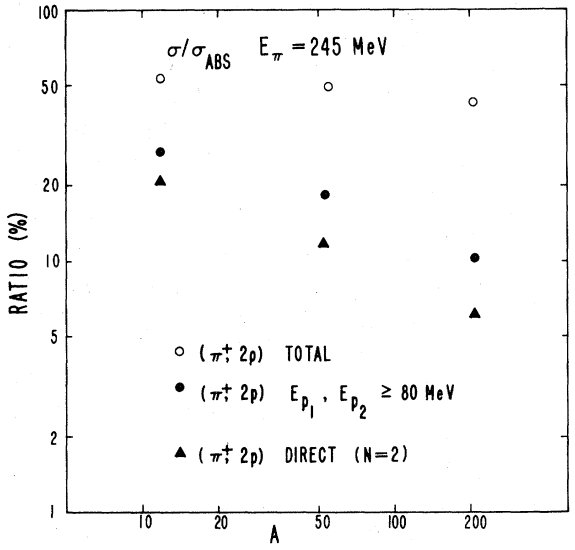

FIG. 10. Calculated partial cross section for the inclusive $(\pi^+,2p)$ process (open circles), the same process with lower limits of 80 MeV on the outgoing protons [which is the experimental limit of Altman *et al.* (Ref. 7)] (full circles), and the direct (exclusive) $(\pi^+,2p)$ reaction (triangles) for 245 MeV π^+ on ^{12}C, ^{56}Fe, and ^{209}Bi targets, shown as fractions of the true absorption cross section.

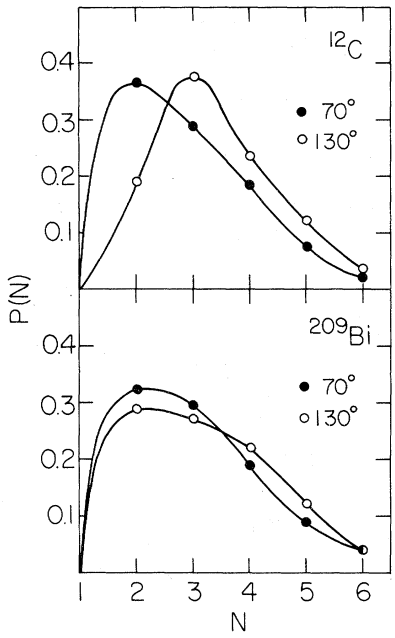

FIG. 11. The probability distribution for the inclusive $(\pi^+,2p)$ reaction for 245 MeV π^+ on ^{12}C and ^{209}Bi as a function of the number of nucleons N which interact with the pion for two angles of one of the emitted protons, $\theta_p = 70°$ (full circles) and $\theta_p = 130°$ (open circles).

result of the increased scattering probability of the pion and the protons.

It was already mentioned that the number of protons taking part in the pion absorption process is of particular interest for the understanding of the pion absorption mechanism in nuclei. The minimum number is $N=2$ [which is the direct or exclusive $(\pi^+,2p)$ reaction shown in Fig. 10 as a ratio of the total absorption cross section], but the pion may interact with additional nucleons before being absorbed. In Fig. 11, we show the probability distribution for the inclusive $(\pi^+,2p)$ reaction as a function of the number of nucleons N which interact with the pion, for the emission angles of one of the protons, $\theta_p = 70°$ and 130°. It is seen that, in general, the distribution $P(N)$ is peaked at $N=2$ but it is quite broad and approximately angle independent, except for ^{12}C, $\theta_p = 130°$ where the peak is shifted to $N=3$ as a result of the smaller probability of the direct $(N=2)$ process at this angle. For ^{209}Bi this effect is compensated by the relatively large proton rescattering probability. Our results are in very good agreement with the calculated results of Masutani and Yazaki[18] for 240 MeV π^+ absorbed in ^{16}O, which are based on an optical model calculation.

C. Possible origins of discrepancies between experimental and calculated results

Our model overestimates the absorption cross section for the upper half of our energy range since it assumes that a Δ resonance is formed in all pion-nucleon collisions, whereas in fact, a sizable fraction of the scattering amplitude in this energy range is nonresonant $(T=\frac{1}{2})$. For the same reason, the inelastic scattering cross section is underestimated for these energies. This may also be one of the reasons for the discrepancies seen in Figs. 1–3 and 8 between the experimental and calculated results.

Of potentially greater theoretical interest may be the discrepancy between our calculated results for the ratio of the $(\pi^-,\pi^-p)/(\pi^+,\pi^+p)$ cross sections shown in Fig. 7 for ^{12}C at 245 MeV and the experimental results. The calculated ratio is larger than the free $(\pi^-,\pi^-p)/(\pi^+,\pi^+p)$ cross section ratio due to final state interactions, particularly (π^-,π^-n) followed by an (n,p) reaction, which constitutes a sizable fraction of the inclusive (π^-,π^-p) cross section whereas the equivalent reaction for π^+ is negligible compared to the direct (π^+,π^+p) reaction.[19,20]

The experimental results[5] show the $(\pi^-,\pi^-p)/(\pi^+,\pi^+p)$ ratio to be *smaller* than the free ratio. It is unlikely that this result can be explained by incoherent effects of the type included in our model. An interpretation of this ratio in terms of destructive interference effects was proposed by Lenz and Moniz.[21]

ACKNOWLEDGMENTS

We wish to acknowledge many illuminating discussions with Dr. D. Ashery, Dr. J. M. Eisenberg, Dr. J. Hüfner, Dr. F. Lenz, and Dr. E. J. Moniz. We wish to thank Mrs. S. Yasur for her help in performing the computations.

[1]K. Chen *et al.*, Phys. Rev. 166, 949 (1968).
[2]K. Chen, G. Friedlander, and J. M. Miller, Phys. Rev. 176, 1208 (1968).
[3]G. D. Harp *et al.*, Phys. Rev. C 8, 581 (1973).
[4]G. D. Harp, Phys. Rev. C 10, 2387 (1974).
[5]E. Piasetzky *et al.*, Phys. Rev. Lett. 46, 1271 (1981).
[6]E. Piasetzky *et al.*, Phys. Rev. C 25, 2687 (1982).
[7]A. Altman *et al.*, contribution to the 9th International Conference on High Energy Physics and Nuclear Structure, Versailles, 1981.
[8]R. D. McKeown *et al.*, Phys. Rev. Lett. 44, 1033 (1980); Phys. Rev. C 24, 211 (1981).
[9]D. Ashery *et al.*, Phys. Rev. C 23, 2173 (1981).
[10]Y. Yariv and Z. Fraenkel, Phys. Rev. C 20, 2227 (1979).
[11]Y. Yariv and Z. Fraenkel, Phys. Rev. C 24, 488 (1981).
[12]J. N. Ginocchio, Phys. Rev. C 17, 195 (1978).
[13]K. Chen, G. Friedlander, G. D. Harp, and J. M. Miller, Phys. Rev. C 4, 2234 (1971).
[14]J. Hüfner and M. C. Nemes, Phys. Rev. C 23, 2538 (1981).
[15]L. R. B. Elton, *Nuclear Sizes* (Oxford University Press, New York, 1961), p. 23.
[16]E. Belloti, S. Bonetti, D. Cavalli, and C. Matteuzzi, Nuovo Cimento 14A, 567 (1973).
[17]E. J. Moniz *et al.*, Phys. Rev. Lett. 26, 445 (1971).
[18]K. Masutani and K. Yazaki, Phys. Lett. 104B, 1 (1981).
[19]P. W. Hewson, Nucl. Phys. A133, 659 (1969).
[20]M. M. Sternheim and R. R. Silbar, Phys. Rev. C 21, 1974 (1980).
[21]F. Lenz and E. J. Moniz (private communication).